Supplemental Material to: "Beating the 3 dB Limit for Intracavity Squeezing and Its Application to Nondemolition Qubit Readout"

Wei Qin,[1] Adam Miranowicz,[1,2] and Franco Nori[1,3,4]

[1] *Theoretical Quantum Physics Laboratory, RIKEN Cluster for Pioneering Research, Wako-shi, Saitama 351-0198, Japan*
[2] *Institute of Spintronics and Quantum Information, Faculty of Physics, Adam Mickiewicz University, 61-614 Poznań, Poland*
[3] *RIKEN Center for Quantum Computing, Wako-shi, Saitama 351-0198, Japan*
[4] *Department of Physics, The University of Michigan, Ann Arbor, Michigan 48109-1040, USA*

Introduction

Here, we first summarize our main results in this work. Next, we recall the 3 dB limit of intracavity squeezing of a semiclassical degenerate parametric amplifier (DPA) to explain the reason for that limit, and accordingly to give the motivation of our method. Subsequently, we present a detailed derivation of the effective Hamiltonian of generating a strong steady-state intracavity squeezing, and discuss its physical interpretation in the laboratory frame. Then, we demonstrate the physical mechanism of beating the 3 dB squeezing limit with our method. Furthermore, we analyze the effects of intracavity squeezing of the semiclassical and fully quantum DPAs on longitudinal qubit readout. Finally, a possible implementation of the intracavity-squeezing enhanced longitudinal qubit readout is discussed.

Click here to see a PDF file with slides about the present work, which is placed in Dropbox.

The supplemental material also contains a pedagogical presentation of this work (see video1 and video2), available for interested readers.

S1. Summary of our main results

Before discussing more technical details, we first summarize the main results of our work in this section. These main results, including some numerical values, are summarized in Table I by comparing intracavity squeezing of the semiclassical and fully quantum DPAs, and their effects on longitudinal qubit readout. More details are described as follows:

TABLE I. Comparison between intracavity squeezing of the semiclassical and fully quantum DPAs, and between their effects on longitudinal qubit readout. Here, $\mathcal{C}$ is the cooperativity of the fully quantum DPA, SNR stands for the signal-to-noise ratio, $\mathrm{SNR}_z^{\mathrm{std}}$ is the SNR of the standard longitudinal readout with no squeezing, ϵ_m is the measurement error, τ is the measurement time, r_p is the degree of intracavity squeezing of the fully quantum DPA, and $r_{\mathrm{out}}^{\mathrm{sc}}$ is the degree of squeezing of the output field of the semiclassical DPA.

DPA type	Steady-state intracavity squeezing	Longitudinal qubit readout					
		$\mathcal{C}$	$\mathrm{SNR}/\mathrm{SNR}_z^{\mathrm{std}}$	$\mathrm{SNR}^{\S}$	ϵ_m	τ (ns)	Degree of squeezing of the measurement noise
semiclassical	limited to 3 dB	—	$\simeq 1^{\dagger}$	1.1	$\simeq 0.22$	$\simeq 53$	τ-dependent
fully quantum	arbitrarily strong	any	$\sqrt{\frac{4\mathcal{C}+1}{4\mathcal{C}\exp(-2r_p)+1}}$	4.7	$\simeq 4.4\times10^{-4}$		τ-independent
		$\gg \frac{1}{4}\exp(2r_p)$	$\simeq \exp(r_p)$	8.9	$\simeq 1.5\times10^{-10}$		

[†] This case of effectively no improvement is observed even for a large $r_{\mathrm{out}}^{\mathrm{sc}}$;
[§] To calculate the SNR values, we assume $r_{\mathrm{out}}^{\mathrm{sc}} = r_p = 2$ ($\simeq 17$ dB), and a modest cooperativity of $\mathcal{C} = 5$.

(1) While intracavity squeezing of a semiclassical DPA is limited, as is well known, to 3 dB in the steady state, we show that our approach can, in principle, lead to an arbitrarily strong steady-state intracavity squeezing by exploiting the pump mode of a fully quantum DPA.

The reason for this sharp contrast is that the photon loss of the signal mode, which is the origin of the 3 dB squeezing limit of the semiclassical DPA, is now engineered as a resource in our approach rather than a noise source.

Our present work is, to our knowledge, the first demonstration of the possibility of exploiting a fully quantum DPA to beat the 3 dB limit for intracavity squeezing.

(2) Furthermore, our strong fully-quantum-DPA intracavity squeezing, which is equivalent to an externally generated and injected squeezed reservoir, can be applied to longitudinal qubit readout. For comparison, we also analyze the effect of the semiclassical-DPA intracavity squeezing on such a readout. We find that these two types of intracavity squeezing exhibit strikingly different performances.

In the semiclassical-DPA case, we find that the degree of squeezing of the measurement noise strongly depends on the measurement time, i.e., it increases from zero as the measurement time increases. This means that a large squeezing of the measurement noise, corresponding to a high readout SNR, needs a long measurement time. Thus, the semiclassical-DPA intracavity squeezing cannot enable a significant increase in the SNR for the short-time measurement of practical interest, even with a strong squeezing of the output field. However, this is not the case when our fully-quantum-DPA intracavity squeezing is used.

We demonstrate that in the fully-quantum-DPA case, the degree of squeezing of the measurement noise is always equal to the degree of intracavity squeezing, and is independent of the measurement time. This enables an exponential increase in the SNR for any measurement time, and leads to an extremely low measurement error, which can be made many orders of magnitude smaller than those obtained in both the semiclassical-DPA case and the standard longitudinal readout with no squeezing.

Having summarized the main results presented in our work, we show more technical details in the following sections.

S2. Limited steady-state intracavity squeezing of the semiclassical degenerate parametric amplifier

In this section, we recall the 3 dB limit of the semiclassical-DPA intracavity squeezing to explain the reason for such a limit, i.e., the photon loss of the signal mode and, accordingly, to give the motivation of our method. We begin with the standard master equation,

$$\dot{\hat{\rho}}_s = -i\left[\hat{H}_{2\mathrm{pd}}, \hat{\rho}_s\right] + \kappa_s \mathcal{L}\left(\hat{a}_s\right)\hat{\rho}_s, \tag{S1}$$

$$\hat{H}_{2\mathrm{pd}} = \Delta_s \hat{a}_s^\dagger \hat{a}_s + \Omega_{2\mathrm{pd}}\left(\hat{a}_s^2 + \mathrm{H.c.}\right), \tag{S2}$$

where $\hat{\rho}_s$ is the density matrix of the signal mode $\hat{a}_s$, $\Delta_s = \omega_s - \omega_d/2$, and $\Omega_{2\mathrm{pd}} = g\alpha_p^{\mathrm{d}}$. Here, ω_s is the frequency of the signal mode, and ω_d is the frequency of the coherent driving of the pump mode of frequency ω_p. Under the master equation, the number of intracavity photons, $\langle \hat{a}_s^\dagger \hat{a}_s \rangle$, and the two-photon-correlation term, $\langle \hat{a}_s \hat{a}_s \rangle$, evolve as

$$\langle \hat{a}_s^\dagger \hat{a}_s \rangle (t) = \frac{8\Omega_{2\mathrm{pd}}^2}{\kappa_s^2 - 4\omega^2} - \mathcal{Q}_0 \exp\left(-\kappa_s t\right), \tag{S3}$$

$$\langle \hat{a}_s \hat{a}_s \rangle (t) = -\frac{2\Omega_{2\mathrm{pd}}\left(2\Delta_s + i\kappa_s\right)}{\kappa_s^2 - 4\omega^2} + \mathcal{Q}_1 \exp\left(-\kappa_s t\right), \tag{S4}$$

where $\omega = \sqrt{4\Omega_{2\mathrm{pd}}^2 - \Delta_s^2}$, and we have defined

$$\mathcal{Q}_0 = \frac{4\Omega_{2\mathrm{pd}}^2}{\omega\left(\kappa_s^2 - 4\omega^2\right)}\left[2\omega\cosh\left(2\omega t\right) + \kappa_s \sinh\left(2\omega t\right)\right], \tag{S5}$$

$$\mathcal{Q}_1 = \frac{2\Omega_{2\mathrm{pd}}}{\omega\left(\kappa_s^2 - 4\omega^2\right)}\left[\omega\left(2\Delta_s + i\kappa_s\right)\cosh\left(2\omega t\right) - \left(i2\Delta_s^2 - \Delta_s\kappa_s - i8\Omega_{2\mathrm{pd}}^2\right)\sinh\left(2\omega t\right)\right]. \tag{S6}$$

To ensure that the system is stable, ω is required to be either a purely imaginary number, or a purely real number but smaller than $\kappa_s/2$. As a consequence, the squeezing parameter,

$$\xi_s^2 = 1 + 2\left(\langle \hat{a}_s^\dagger \hat{a}_s \rangle - \left|\langle \hat{a}_s \hat{a}_s \rangle\right|\right), \tag{S7}$$

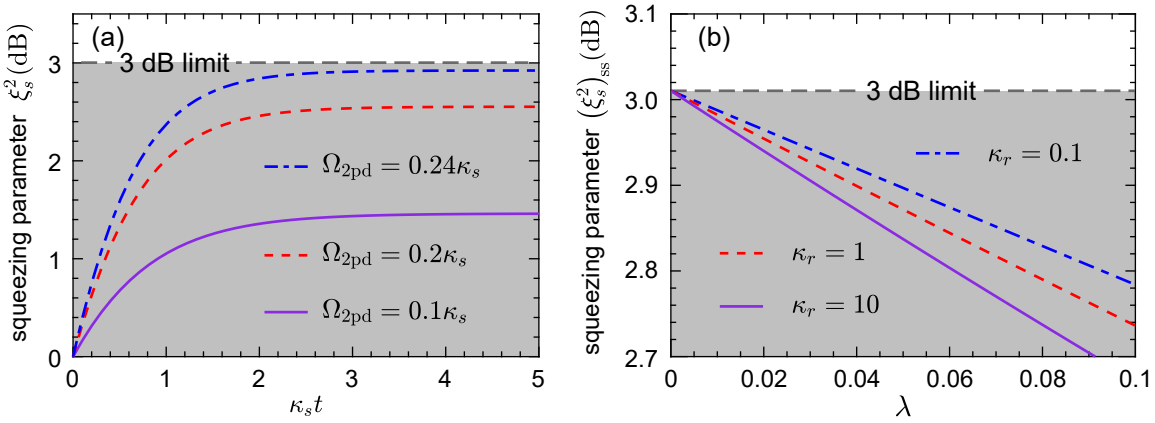

FIG. S1. (a) Upper-bounded steady-state intracavity squeezing of the semiclassical degenerate parametric amplifier. Here, we set $\Delta_s = 0$ as an example, so that the steady-state squeezing of the signal mode $\hat{a}_s$ approaches the 3 dB limit as $\Omega_{2\mathrm{pd}} \to \kappa_s/4$. Note that when $\Omega_{2\mathrm{pd}} > \kappa_s/4$, the system becomes unstable. (b) Effects of nonlinear corrections from the residual coupling $\hat{V}$ on the steady-state intracavity squeezing, calculated according to the formalism of Ref. [S1] for $\delta = -\lambda\sqrt{(2+3\kappa_r)/(2+\kappa_r)}/2$. As $\lambda \to 0$, the steady-state intracavity squeezing increases to the 3 dB limit. In both panels, the gray shaded areas refer to the regime below the 3 dB limit. Note that especially in panel (b), the position of the 3 dB limit is slightly greater than 3 dB, due to the fact that $-10\log_{10}(0.5) \simeq 3.01$.

in the steady state ($t \to \infty$) is found to be

$$\left(\xi_s^2\right)_{\mathrm{ss}} = \frac{1}{1+\mu}, \tag{S8}$$

where

$$\mu = \frac{4\Omega_{2\mathrm{pd}}}{\sqrt{\kappa_s^2 - 4\omega^2 + \left(4\Omega_{2\mathrm{pd}}\right)^2}}. \tag{S9}$$

It is clear that $\mu < 1$, and thus that as shown in Fig. S1(a), the minimum $\left(\xi_s^2\right)_{\mathrm{ss}}$ is limited to 0.5, corresponding to the 3 dB limit.

In the above discussion, we have neglected the residual nonlinear coupling,

$$\hat{V} = g\left(\hat{a}_s^2\hat{a}_p^\dagger + \mathrm{H.c.}\right). \tag{S10}$$

The effect of this residual coupling on intracavity squeezing has been considered in Ref. [S1] for $\omega_d = \omega_p = 2\omega_s$. It was shown in Ref. [S1] that when the nonlinear corrections from the residual coupling $\hat{V}$ are taken into account, the steady-state squeezing parameter in Eq. (S8) becomes

$$\left(\xi_s^2\right)_{\mathrm{ss}} = \frac{1}{1+\mu} + \frac{\lambda^2\mu}{2\left(1+\mu\right)^2\left(1-\mu\right)}\left\{\frac{\mu\kappa_r}{\kappa_r+2} + \frac{\kappa_r\left(1-\mu+\mu^2\right)+2\left(1+\mu\right)}{\left(1+\mu\right)\left[\kappa_r+2\left(1+\mu\right)\right]}\right\}, \tag{S11}$$

where $\lambda = 4g/\sqrt{2\kappa_p\kappa_s}$ and $\kappa_r = \kappa_p/\kappa_s$.

Because $\left(\xi_s^2\right)_{\mathrm{ss}}$ in Eq. (S11) becomes divergent as $\mu \to 1$, we can now rewrite μ as $\mu = 1+\delta$, with $\delta \lesssim 0$, yielding

$$\left(\xi_s^2\right)_{\mathrm{ss}} = \frac{1}{2+\delta} - \frac{\lambda^2\left(1+\delta\right)}{2\delta\left(2+\delta\right)^2}\left[\frac{\kappa_r\left(1+\delta\right)}{2+\kappa_r} + \frac{4+\kappa_r+\left(2+\kappa_r\right)\delta+\kappa_r\delta^2}{\left(2+\delta\right)\left(4+\kappa_r+2\delta\right)}\right]. \tag{S12}$$

We find, according to Eq. (S12), that when

$$\delta = -\frac{\lambda}{2}\sqrt{\frac{2+3\kappa_r}{2+\kappa_r}}, \quad \text{and} \quad \lambda \to 0, \tag{S13}$$

the squeezing parameter $\left(\xi_s^2\right)_{\mathrm{ss}}$ reaches its minimum value 0.5. This indicates that, as numerically confirmed in Fig. S1(b), the steady-state intracavity squeezing is still limited to 3 dB, even with the inclusion of the nonlinear contributions from the residual coupling $\hat{V}$.

Furthermore, we find from Fig. S1(b) that $\left(\xi_s^2\right)_{\rm ss}$ decreases from the 3 dB limit, as the parameter λ, which determines the ratio of nonlinear-to-linear rates of change, increases from zero. This means that the nonlinear corrections from the residual coupling $\hat{V}$ lead to a decrease, rather than an increase, of the degree of intracavity squeezing. There are two reasons for such a decrease:

- First, when the nonlinear contributions from $\hat{V}$ are considered, there exists some entanglement between the pump and signal modes, such that the squeezed state of the signal mode becomes more mixed, thus further reducing the degree of squeezing.

- Second, the signal-mode photons can be up-converted into the pump mode by the residual coupling $\hat{V}$, and then can be lost via the photon loss of the pump mode. This gives rise to a two-photon loss process, which can also destroy the desired squeezing.

The 3 dB squeezing limit is essentially attributed to the cavity photon loss (i.e., the photon loss of the signal mode), which destroys the essence of squeezing, i.e., two-photon correlations [represented by the term $\langle \hat{a}_s \hat{a}_s \rangle$ in Eq. (S7)]. This can be physically understood as follows. The two-photon driving $\Omega_{\rm 2pd}$ injects correlated photon pairs into the cavity, so theoretically generating perfect two-photon correlations. Therefore, if there is no cavity photon loss, the two-photon driving can generate an ideal, arbitrarily strong intracavity squeezing. However, the cavity photon loss is always present, such that single photons of some correlated photon pairs leak out of the cavity, thus leading to a partial loss of two-photon correlations. Consequently, intracavity squeezing is lost partially and is ultimately limited to 3 dB in the steady state.

Therefore, the motivation of our method to beat the 3 dB limit is to turn the signal-mode photon loss from a noise source into a resource via quantum reservoir engineering. We find that with a fully quantum DPA, the signal-mode photon loss, when exploited as a resource, can steer the pump mode into a squeezed steady state. More importantly, we find that the signal-mode photon loss can strongly suppress the detrimental effect of the pump-mode photon loss on squeezing, and ultimately, an arbitrarily strong steady-state squeezing of the pump mode can be achieved. The underlying physical mechanism is discussed in Sec. S5.

S3. Detailed derivation of the effective Hamiltonian

Below, we give a detailed derivation of the effective Hamiltonian $\hat{H}_{\rm eff}$. To begin, we consider the original Hamiltonian $\hat{H} = \hat{H}_0 + \hat{H}_{\rm 2td}$, where $\hat{H}_0$ and $\hat{H}_{\rm 2td}$ are given in Eqs. (1) and (2), respectively, in the main article. In terms of the signal Bogoliubov mode $\hat{\beta}_s$, the Hamiltonian $\hat{H}$ is reexpressed as

$$\hat{H} = \hat{\mathcal{H}} + \hat{R}_1 + \hat{R}_1^\dagger + \hat{R}_2 + \hat{R}_2^\dagger, \tag{S14}$$

$$\begin{aligned}\hat{\mathcal{H}} = {} & \Delta_p \hat{a}_p^\dagger \hat{a}_p + \Lambda_s \hat{\beta}_s^\dagger \hat{\beta}_s + g_0 \hat{\beta}_s^\dagger \hat{\beta}_s \left(\hat{a}_p + \hat{a}_p^\dagger\right) \\ & + \cosh\left(r_s\right) \sum_{k=\pm} \left(\mathcal{E}_k \hat{\beta}_s^\dagger e^{-i\omega_k t} + \text{H.c.}\right),\end{aligned} \tag{S15}$$

$$\hat{R}_1 = g\left[\cosh^2\left(r_s\right)\hat{\beta}_s^2 + \sinh^2\left(r_s\right)\hat{\beta}_s^{\dagger 2}\right]\hat{a}_p^\dagger, \tag{S16}$$

$$\hat{R}_2 = -\sinh\left(r_s\right) \sum_{k=\pm} \mathcal{E}_k \hat{\beta}_s e^{-i\omega_k t}. \tag{S17}$$

Here, $\hat{R}_1$ and $\hat{R}_2$ are the residual components of the parametric coupling g and the two-tone driving $\Omega_{\rm 2td}$, respectively. Correspondingly, the master equation is given by

$$\begin{aligned}\dot{\hat{\rho}} = {} & -i\left[\hat{H}, \hat{\rho}\right] + \kappa_p \mathcal{L}\left(\hat{a}_p\right)\hat{\rho} + \kappa_s \cosh^2\left(r_s\right)\mathcal{L}\left(\hat{\beta}_s\right)\hat{\rho} \\ & + \kappa_s \sinh^2\left(r_s\right)\mathcal{L}\left(\hat{\beta}_s^\dagger\right)\hat{\rho} - \frac{1}{2}\kappa_s \sinh\left(2r_s\right)\mathcal{D}\left(\hat{\beta}_s\right)\hat{\rho} - \frac{1}{2}\kappa_s \sinh\left(2r_s\right)\mathcal{D}\left(\hat{\beta}_s^\dagger\right)\hat{\rho},\end{aligned} \tag{S18}$$

where $\mathcal{L}\left(\hat{o}\right)\hat{\rho} = \hat{o}\hat{\rho}\hat{o}^\dagger - \frac{1}{2}\left(\hat{o}^\dagger\hat{o}\hat{\rho} + \hat{\rho}\hat{o}^\dagger\hat{o}\right)$, and $\mathcal{D}\left(\hat{o}\right)\hat{\rho} = \hat{o}\hat{\rho}\hat{o} - \frac{1}{2}\left(\hat{o}\hat{o}\hat{\rho} + \hat{\rho}\hat{o}\hat{o}\right)$.

In order to derive $\hat{H}_{\rm eff}$, let us first focus our attention on the term $\hat{\mathcal{H}}$, which provides the dominant contribution to the generation of intracavity squeezing. We then analyze the terms $\hat{R}_1$ and $\hat{R}_2$, both of which, as purely high-frequency effects, can be dropped by properly compensating some resonance shifts of the modes $\hat{\beta}_s$ and $\hat{a}_p$.

To proceed, we introduce a displacement operator, $\hat{D}_p(\alpha_p) = \exp\left(\alpha_p \hat{a}_p^\dagger - \alpha_p^\dagger \hat{a}_p\right)$, for the mode $\hat{a}_p$, and a time-dependent displacement operator, $\hat{D}_s[\alpha_s(t)] = \exp\left[\alpha_s(t)\,\hat{\beta}_s^\dagger - \alpha_s^*(t)\,\hat{\beta}_s\right]$, for the mode $\hat{\beta}_s$, such that

$$\hat{D}_p^\dagger(\alpha_p)\,\hat{a}_p\hat{D}_p(\alpha_p) = \hat{a}_p + \alpha_p, \tag{S19}$$

$$\hat{D}_s^\dagger[\alpha_s(t)]\,\hat{\beta}_s\hat{D}_s[\alpha_s(t)] = \hat{\beta}_s + \alpha_s(t), \tag{S20}$$

where $\alpha_s(t) = \alpha_s^+ e^{-i\omega_+ t} + \alpha_s^- e^{-i\omega_- t}$. Here, α_p is the overall field amplitude of the mode $\hat{a}_p$, induced by the $\omega_\pm$ tones (i.e., the $\omega_\pm^{\rm d}$ tones in the original lab frame), while $\alpha_s^\pm$ are the field amplitudes of the mode $\hat{\beta}_s$, induced by the $\omega_\pm$ tones, respectively.

When applying the displacement transformations in Eqs. (S19) and (S20), a displaced $\hat{\mathcal{H}}$ is found to be

$$\begin{aligned}\hat{\mathcal{H}}_{\rm disp} = {}& \hat{U}^\dagger(t)\,\hat{\mathcal{H}}\hat{U}(t) - i\hat{U}^\dagger(t)\,\dot{\hat{U}}(t) \\ & - i\frac{1}{2}\kappa_p\left(\alpha_p\hat{a}_p^\dagger - \text{H.c.}\right) - i\frac{1}{2}\kappa_s\left[\alpha_s(t)\,\hat{\beta}_s^\dagger - \text{H.c.}\right],\end{aligned} \tag{S21}$$

where $\hat{U}(t) = \hat{D}_p(\alpha_p)\,\hat{D}_s[\alpha_s(t)]$. It then follows, using

$$\begin{aligned}\dot{\hat{U}}(t) = {}& \hat{D}_p(\alpha_p)\,\hat{D}_s[\alpha_s(t)] \\ & \times\left\{\frac{1}{2}\frac{d}{dt}|\alpha_s(t)|^2 - i\left(\omega_+\alpha_s^{+*}e^{i\omega_+ t} + \omega_-\alpha_s^{-*}e^{i\omega_- t}\right)\left[\hat{\beta}_s + \alpha_s(t)\right]\right. \\ & \left. - i\left(\omega_+\alpha_s^+ e^{-i\omega_+ t} + \omega_-\alpha_s^- e^{-i\omega_- t}\right)\hat{\beta}_s^\dagger\right\},\end{aligned} \tag{S22}$$

that

$$\begin{aligned}\hat{\mathcal{H}}_{\rm disp} = {}& \Delta_p\hat{a}_p^\dagger\hat{a}_p + \Lambda_s\hat{\beta}_s^\dagger\hat{\beta}_s + g_0\hat{\beta}_s^\dagger\hat{\beta}_s\left(\hat{a}_p + \hat{a}_p^\dagger\right) \\ & + g_0\left(\alpha_s^+\hat{\beta}_s^\dagger e^{-i\omega_+ t} + \text{H.c.}\right)\left(\hat{a}_p + \hat{a}_p^\dagger\right) + g_0\left(\alpha_s^-\hat{\beta}_s^\dagger e^{-i\omega_- t} + \text{H.c.}\right)\left(\hat{a}_p + \hat{a}_p^\dagger\right) \\ & + g_0\left[\alpha_s^-\left(\alpha_s^+\right)^* e^{i(\omega_+ - \omega_-)t} + \text{H.c.}\right]\left(\hat{a}_p + \hat{a}_p^\dagger\right),\end{aligned} \tag{S23}$$

where we have set

$$\alpha_p = g_0\frac{|\alpha_s^+|^2 + |\alpha_s^-|^2}{i\kappa_p/2 - \Delta_p}, \quad \text{and} \quad \alpha_s^\pm = \frac{\cosh(r_s)\,\mathcal{E}_\pm}{i\kappa_s/2 - \Lambda_s + \omega_\pm}. \tag{S24}$$

Note that here, the resonance shift, $2g_0\text{Re}[\alpha_p]$, of the mode $\hat{\beta}_s$ has been absorbed into Λ_s. Under the assumption of $\omega_\pm = \Lambda_s \pm \Delta_p$, we can drop high-frequency components and then obtain the effective Hamiltonian in the rotating frame of reference of $\hat{h} = \Delta_p\hat{a}_p^\dagger\hat{a}_p + \Lambda_s\hat{\beta}_s^\dagger\hat{\beta}_s$ as follows:

$$\hat{H}_{\rm eff} = G_-\hat{\beta}_s^\dagger\hat{a}_p + G_+\hat{\beta}_s^\dagger\hat{a}_p^\dagger + \text{H.c.} \tag{S25}$$

$$= \mathcal{G}\left(\hat{\beta}_p\hat{\beta}_s^\dagger + \hat{\beta}_p^\dagger\hat{\beta}_s\right), \tag{S26}$$

where $G_\pm = g_0\alpha_s^\pm$ and $\mathcal{G} = \sqrt{G_-^2 - G_+^2}$. Here, we have set the field amplitudes $\alpha_s^\pm$ to be real, for simplicity, and have defined a Bogoliubov mode for the pump mode,

$$\hat{\beta}_p = \hat{a}_p\cosh(r_p) + \hat{a}_p^\dagger\sinh(r_p), \tag{S27}$$

with $\tanh(r_p) = G_+/G_-$.

Now consider the term $\hat{R}_1$. We apply the displacement transformations in Eqs. (S19) and (S20) to $\hat{R}_1$, and see that $\hat{R}_1$ becomes

$$\hat{R}_{1,\rm disp} = g\left[\cosh^2(r_s)\,\hat{\Pi} + \sinh^2(r_s)\,\hat{\Pi}^\dagger\right]\left(\hat{a}_p^\dagger + \alpha_p^*\right), \tag{S28}$$

with

$$\hat{\Pi} = \hat{\beta}_s^2 + 2\hat{\beta}_s \sum_{k=\pm} \alpha_s^k e^{-i\omega_k t} + \left(\sum_{k=\pm} \alpha_s^k e^{-i\omega_k t} \right)^2 . \tag{S29}$$

As assumed in the main article, the degree, r_s, of squeezing of the signal mode $\hat{a}_s$ is very small, so that the terms in Eq. (S28), which are proportional to $\sinh^2(r_s)$, can be dropped, yielding

$$\hat{R}_{1,\mathrm{disp}} \simeq g_c \hat{\Pi} \left(\hat{a}_p^\dagger + \alpha_p^* \right) + \mathrm{H.c.}, \tag{S30}$$

where $g_c = g \cosh^2(r_s) \simeq g$. The coupling $\hat{R}_{1,\mathrm{disp}}$ is dominated by the couplings,

$$\hat{P} = 2 g_c \hat{\beta}_s a_p^\dagger \sum_{k=\pm} \alpha_s^k e^{-i\omega_k t} + \mathrm{H.c.}, \tag{S31}$$

$$\hat{Q} = g_c \left(\sum_{k=\pm} \alpha_s^k e^{-i\omega_k t} \right)^2 \hat{a}_p^\dagger + \mathrm{H.c.} \tag{S32}$$

Using the formalism of Ref. [S2] shows that, under the resonance conditions $\omega_\pm = \Lambda_s \pm \Delta_p$, the dynamics of the coupling $\hat{P}$ effectively causes a resonance up-shift of

$$\delta_{\mathrm{shift}} = 2 g_c^2 \left[\frac{1}{\Lambda_s} \left(\alpha_s^+ \right)^2 + \frac{1}{\Lambda_s - \Delta_p} \left(\alpha_s^- \right)^2 \right] \tag{S33}$$

for the mode $\hat{\beta}_s$, and also a resonance down-shift of the same amount for the mode $\hat{a}_p$. These two shifts can be compensated by slightly modifying the resonance condition $\omega_- = \Lambda_s - \Delta_p$ to be $\omega_- = \Lambda_s - \Delta_p + 2\delta_{\mathrm{shift}}$.

On the other hand, the coupling $\hat{Q}$ can be simply viewed as a detuned three-tone driving of the mode $\hat{a}_p$. To cancel its effect, a direct method is to drive the mode $\hat{a}_p$ using another opposite-phase three-tone driving. But to simplify this problem, we note that recently, a strong single-photon parametric coupling has been experimentally realized, with the strength g being able to range from some tens of kHz to some tens of MHz [S3–S10]. This indicates that even when the intracavity-field amplitudes $\alpha_s^\pm$ are small [e.g., $\alpha_s^\pm \sim 1$ as in Fig. 1(b)], a large $\mathcal{C}$ can still be achieved. Here, $\mathcal{C} = \mathcal{G}^2/(\kappa_s \kappa_p)$ is a key factor, whose larger value can lead to a stronger intracavity squeezing as discussed in the main article. Thus in this case, the coupling $\hat{Q}$ acts as a high-frequency component. At the same time, the residual driving term $\hat{R}_2$ can also be treated as a high-frequency component, because for $r_s \ll 1$ we can have $(\omega_\pm + \Lambda_s) \gg \sinh(r_s)\, \mathcal{E}_\pm$. Consequently, both the terms $\hat{Q}$ and $\hat{R}_2$ are allowed to be directly dropped. Such is the case considered in the main article.

By the above analysis, it is seen that the coherent dynamics of the three-tone driven DPA, which is described exactly by the Hamiltonian $\hat{H}$, can be well governed by the effective Hamiltonian $\hat{H}_{\mathrm{eff}}$. This is numerically confirmed in Fig. 1(b) in the main article.

S4. Physical interpretation of the effective Hamiltonian $\hat{H}_{\mathrm{eff}}$ in the laboratory frame.

The effective Hamiltonian $\hat{H}_{\mathrm{eff}}$ in Eq. (S26) models a beam-splitter-type interaction between the signal and pump Bogoliubov modes, but *in the squeezed frame*. Below, we discuss how to understand this effective Hamiltonian *in the laboratory frame*. To be more specific, we first note that the signal Bogoliubov mode $\hat{\beta}_s$ in the squeezed frame, whose resonance frequency is $\Lambda_s = \sqrt{\Delta_s^2 - 4\Omega_{2\mathrm{pd}}^2}$, in fact corresponds to the shifted (or dressed) signal mode in the laboratory frame, whose resonance frequency is $\omega_s^{\mathrm{sq}} = \omega_d/2 + \Lambda_s$. In the laboratory frame, $\hat{H}_{\mathrm{eff}}$ can be rewritten as

$$\hat{H}_{\mathrm{eff}} = \hat{H}_{\mathrm{BST}} + \hat{H}_{\mathrm{TMS}}, \tag{S34}$$

$$\hat{H}_{\mathrm{BST}} = G_- \left(\hat{a}_p \hat{\beta}_s^\dagger + \hat{a}_p^\dagger \hat{\beta}_s \right), \tag{S35}$$

$$\hat{H}_{\mathrm{TMS}} = G_+ \left(\hat{a}_p \hat{\beta}_s + \hat{a}_p^\dagger \hat{\beta}_s^\dagger \right). \tag{S36}$$

Here, $\hat{H}_{\mathrm{BST}}$ and $\hat{H}_{\mathrm{TMS}}$ describe a resonant beam-splitter-type interaction and a resonant two-mode-squeezing interaction, respectively. Thus, the physical interpretation of $\hat{H}_{\mathrm{eff}}$ can be understood as two four-wave-mixing processes, as schematically depicted in Fig. S2.

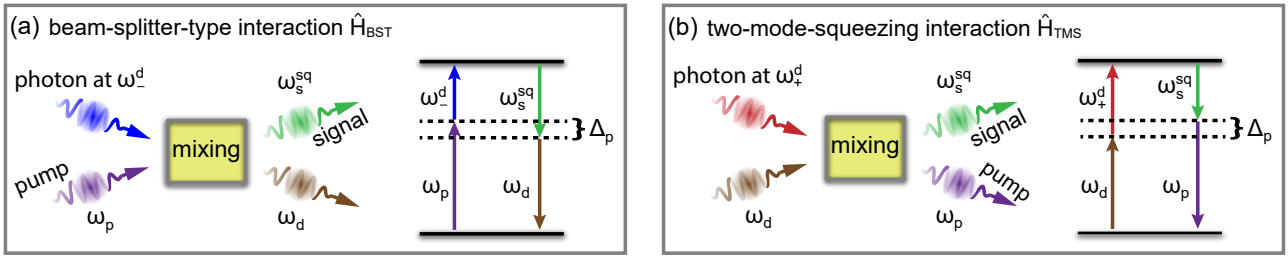

FIG. S2. Four-wave-mixing processes responsible for (a) the beam-splitter-type [i.e., $\hat{H}_{\rm BST}$ in Eq. (S35)] and (b) two-mode-squeezing [i.e., $\hat{H}_{\rm TMS}$ in Eq. (S36)] interactions in the laboratory frame. On the right of both panels is the schematic representation of energy conservation, showing the resonance conditions of these interactions, $\omega_\pm = \Lambda_s \pm \Delta_p$. The beam-splitter-type interaction models the conversion of a photon from the pump mode $\hat{a}_p$ at ω_p into the signal Bogoliubov mode (i.e., the shifted signal mode) $\hat{\beta}_s$ at $\omega_s^{\rm sq}$, which is accompanied by absorbing an $\omega_-^{\rm d}$ photon and emitting another ω_d photon. In contrast, the two-mode-squeezing interaction models the simultaneous creation of two photons in the signal Bogoliubov and pump modes, along with the simultaneous annihilation of an $\omega_+^{\rm d}$ photon and an ω_d photon.

The beam-splitter-type interaction $\hat{H}_{\rm BST}$ in Eq. (S35) exchanges a single photon between the signal Bogoliubov mode $\hat{\beta}_s$ at $\omega_s^{\rm sq}$ and the pump mode $\hat{a}_p$ at ω_p. This process is obtained under the resonance condition $\omega_- = \Lambda_s - \Delta_p$, which, in the laboratory frame, is

$$\omega_-^{\rm d} + \omega_p = \omega_s^{\rm sq} + \omega_d. \tag{S37}$$

It is seen that the beam-splitter-type interaction $\hat{H}_{\rm BST}$ originates from a four-wave-mixing process, which is stimulated by the driving tones at $\omega_-^{\rm d}$ and ω_d. According to the photon description of this process [see Fig. S2(a)], a pump photon at ω_p is down-converted to the mode $\hat{\beta}_s$ at $\omega_s^{\rm sq}$, while annihilating a driving photon at $\omega_-^{\rm d}$ and creating another driving photon at ω_d.

On the other hand, the two-mode-squeezing interaction $\hat{H}_{\rm TMS}$ in Eq. (S36) describes the simultaneous annihilation and creation of two photons in the signal Bogoliubov mode $\hat{\beta}_s$ and the pump mode $\hat{a}_p$. Its resonance condition is $\omega_+ = \Lambda_s + \Delta_p$, which, in the laboratory frame, reads

$$\omega_+^{\rm d} + \omega_d = \omega_s^{\rm sq} + \omega_p. \tag{S38}$$

This implies that the driving tones at $\omega_+^{\rm d}$ and ω_d simulate a four-wave-mixing process [see Fig. S2(b)]. In the photon description, a photon pair of the signal Bogoliubov and pump modes can be created by annihilating two driving photons at $\omega_+^{\rm d}$ and ω_d.

S5. Physical mechanism of beating the 3 dB squeezing limit

Having given a physical interpretation of the effective Hamiltonian $\hat{H}_{\rm eff}$ in Sec. S4, we here show in detail the physical mechanism of beating the 3 dB squeezing limit with our proposal. The basic idea of our proposal is to apply a two-tone driving to the signal mode, in addition to the usual driving of the pump mode. In order to show the underlying physical mechanism explicitly, we consider the effective master equation,

$$\dot{\hat{\rho}} = -i\left[\hat{H}_{\rm eff}, \hat{\rho}\right] + \kappa_p \mathcal{L}\left(\hat{a}_p\right)\hat{\rho} + \kappa_s \mathcal{L}(\hat{\beta}_s)\hat{\rho}. \tag{S39}$$

In an ideal case of $\kappa_p = 0$, the photon loss of the mode $\hat{\beta}_s$ can cool the mode $\hat{\beta}_p$ to its ground state, i.e., the ideal squeezed vacuum state expressed as

$$|\Phi_{\rm sv}\rangle = \frac{1}{\sqrt{\cosh\left(r_p\right)}} \sum_{n=0}^{\infty} \frac{\sqrt{(2n)!}}{2^n\, n!} \left[-\tanh\left(r_p\right)\right]^n |2n\rangle, \tag{S40}$$

in terms of photon-number states of the pump mode $\hat{a}_p$. According to Eq. (S40), the state $|\Phi_{\rm sv}\rangle$ is a superposition of only even photon-number states and, thus, has even photon-number parity. We also note that, the state $|\Phi_{\rm sv}\rangle$ is simply the zero photon-number state, $|0\rangle_{\hat{\beta}_p}$, of the mode $\hat{\beta}_p$, such that

$$\hat{\beta}_p|\Phi_{\rm sv}\rangle = \hat{\beta}_p|0\rangle_{\hat{\beta}_p} = 0. \tag{S41}$$

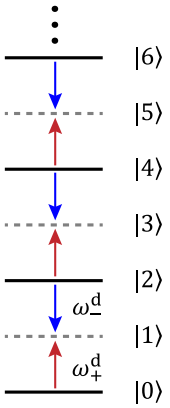

FIG. S3. Schematic of destructive interference leading to an arbitrary steady-state intracavity squeezing. There always exist two different transitions to any odd photon-number state of the signal mode, which are driven by the $\omega_\pm^{\mathrm{d}}$ tones (red and blue arrows), respectively. A squeezed steady state, with an arbitrarily high degree of squeezing, can be achieved since these two transitions can interfere destructively, so that the populations of all the odd photon-number states are zero in the steady state.

Furthermore, the state $|\Phi_{\mathrm{sv}}\rangle$ is a unique steady state, and can be reached from any state of the mode $\hat{a}_p$. The reason is that any state of the mode $\hat{a}_p$ can be expressed in terms of the ground and excited states of the mode $\hat{\beta}_p$, but of these, all the excited states (i.e., all the nonzero photon-number states of the mode $\hat{\beta}_p$) are depopulated by the loss of the mode $\hat{\beta}_s$ in the steady state, leaving only the ground state $|0\rangle_{\hat{\beta}_p}$, i.e., the state $|\Phi_{\mathrm{sv}}\rangle$.

We now consider the effect of the photon loss of the mode $\hat{a}_p$ in the case of $\kappa_p \neq 0$. The desired steady-state squeezing is independent of the initial state of the mode $\hat{a}_p$, as discussed above. This enables the detrimental effect of the photon loss of the mode $\hat{a}_p$ on squeezing to be strongly suppressed, as long as $\kappa_s \gg \kappa_p$. Such a dissipative suppression can be understood from the quantum jump approach. The action of the quantum jump operator $\hat{a}_p$ on the state $|\Phi_{\mathrm{sv}}\rangle$, corresponding to a single-photon loss event, yields

$$\hat{a}_p|\Phi_{\mathrm{sv}}\rangle = -\sinh(r_p)\,|1\rangle_{\hat{\beta}_p}, \tag{S42}$$

where $|1\rangle_{\hat{\beta}_p}$ is the single photon-number state of the mode $\hat{\beta}_p$. It is seen that a single-photon loss event completely destroys the desired squeezing. Despite this, the strong photon loss of the mode $\hat{\beta}_s$ can autonomously steer the state $|1\rangle_{\hat{\beta}_p}$ back to the ground state $|0\rangle_{\hat{\beta}_p}$, i.e., the state $|\Phi_{\mathrm{sv}}\rangle$. Therefore, this strong suppression of the detrimental effect of the photon loss of the mode $\hat{a}_p$ on squeezing is the physical reason why our proposal can beat the 3 dB squeezing limit.

Let us now discuss the role of the two driving tones, at $\omega_\pm^{\mathrm{d}}$, of the signal mode in our proposal. Their role is to form the Bogoliubov mode $\hat{\beta}_p$ in Eq. (S27), which involves the annihilation operator $\hat{a}_p$ and the creation operator $\hat{a}_p^\dagger$ simultaneously. In terms of photon-number states of the pump mode $\hat{a}_p$, the action of the operator $\hat{\beta}_p$, which is triggered by the photon loss of the mode $\hat{\beta}_s$, causes two different transitions to any odd photon-number state, as shown in Fig. S3. One of them, i.e., $|2n\rangle \to |2n+1\rangle$ [corresponding to the action of the operator $\hat{a}_p^\dagger$ in Eq. (S27)], is driven by the tone at ω_+^{d}, and the other transition, i.e., $|2n+2\rangle \to |2n+1\rangle$ [corresponding to the action of the operator $\hat{a}_p$ in Eq. (S27)], is driven by the tone at ω_-^{d}. To satisfy Eq. (S41), destructive interference between these two transitions is required to ensure that all the odd photon-number states are unpopulated in the steady state. In fact, the squeezed steady state $|\Phi_{\mathrm{sv}}\rangle$ is generated by the repeated action of the operator $\hat{\beta}_p$ on the pump mode, which can be initially in any state, until such destructive interference is formed in the steady state. The condition for destructive interference can also be used to derive the coefficients in Eq. (S40). Thus, the role of the two-tone driving is to provide two different transition pathways, which are crucial to form a strong steady-state squeezing.

S6. Longitudinal qubit readout using the semiclassical-DPA intracavity squeezing

In this section, we consider the longitudinal readout of a qubit embedded in the semiclassical DPA, where the pump mode is treated as a classical field and, in turn, as a nonlinear two-photon driving of the signal mode. Specifically, we derive and analyze in detail the measurement signal, measurement noise, and SNR. For a semiclassical DPA, its

intracavity squeezing is limited to 3 dB, but at the same time an arbitrarily strong squeezing can, in principle, be achieved for its output field. It thus seems, at first glance, as though the semiclassical-DPA intracavity squeezing might be suitable to improve longitudinal qubit readout. However, below we demonstrate that *for the short-time measurement, the SNR does not benefit from the semiclassical-DPA intracavity squeezing, even though squeezing of the output field is very strong.* Furthermore, we also demonstrate that *although there is an exponential improvement in the SNR for the long-time measurement, the required measurement time is extremely long and, therefore, is infeasible experimentally.*

To begin, we assume that the qubit to be measured is longitudinally coupled to the signal mode $\hat{a}_s$, as described by the Hamiltonian,

$$\hat{H}_z^{\mathrm{sc}} = \Omega_{2\mathrm{pd}} \left(\hat{a}_s^2 e^{-i2\phi_{2\mathrm{pd}}} + \hat{a}_s^{\dagger 2} e^{i2\phi_{2\mathrm{pd}}} \right) + \chi_z \hat{\sigma}_z \left(\hat{a}_s e^{-i\phi_z} + \hat{a}_s^{\dagger} e^{i\phi_z} \right), \tag{S43}$$

where $\hat{\sigma}_z$ is the Pauli matrix of the qubit. The first term accounts for the semiclassical DPA with a two-photon driving of strength $\Omega_{2\mathrm{pd}}$ and phase $2\phi_{2\mathrm{pd}}$, and the second term for the longitudinal qubit-field coupling of strength χ_z and phase ϕ_z. The longitudinal coupling generates a linear displacement of the signal mode $\hat{a}_s$, conditional on the qubit state. Under $\hat{H}_z^{\mathrm{sc}}$, the quantum Langevin equation of motion for the signal mode $\hat{a}_s$ is

$$\dot{\hat{a}}_s = -i\sigma\chi_z e^{i\phi_z} - \frac{\kappa_s}{2}\hat{a}_s - i2\Omega_{2\mathrm{pd}}\hat{a}_s^{\dagger} e^{i2\phi_{2\mathrm{pd}}} - \sqrt{\kappa_s}\hat{a}_{s,\mathrm{in}}(t). \tag{S44}$$

Here, the qubit has been assumed to be in a definite state, such that the operator $\hat{\sigma}_z$ has been written as a c-number $\sigma = \pm 1$, corresponding to the excited and ground states of the qubit, respectively. This equation of motion can be solved using a formal integration, and the resulting expression for $\hat{a}_s(t)$ is

$$\begin{aligned}
\hat{a}_s(t) = {} & \cosh\left[2\Omega_{2\mathrm{pd}}(t-t_0)\right] \hat{a}_s(t_0)\, e^{-\kappa_s(t-t_0)/2} \\
& - ie^{i2\phi_{2\mathrm{pd}}} \sinh\left[2\Omega_{2\mathrm{pd}}(t-t_0)\right] \hat{a}_s^{\dagger}(t_0)\, e^{-\kappa_s(t-t_0)/2} \\
& - \sqrt{\kappa_s} \int_{t_0}^{t} ds \cosh\left[2\Omega_{2\mathrm{pd}}(t-s)\right] \left[\hat{a}_{s,\mathrm{in}}(t) + ie^{i\phi_z}\sigma\chi_z/\sqrt{\kappa_s}\right] e^{-\kappa_s(t-s)/2} \\
& + ie^{i2\phi_{2\mathrm{pd}}}\sqrt{\kappa_s} \int_{t_0}^{t} ds \sinh\left[2\Omega_{2\mathrm{pd}}(t-s)\right] \left[\hat{a}_{s,\mathrm{in}}^{\dagger}(t) - ie^{-i\phi_z}\sigma\chi_z/\sqrt{\kappa_s}\right] e^{-\kappa_s(t-s)/2},
\end{aligned} \tag{S45}$$

where t_0 is the initial time of the measurement. It is seen that in the case of $\Omega_{2\mathrm{pd}} > \kappa_s/4$, the amplitude of $\hat{a}_s$ increases exponentially with time, and the system becomes unstable. Thus, in order for the system to be stable, we restrict our discussion to the case where $\Omega_{2\mathrm{pd}} < \kappa_s/4$. Note that the special case of $\Omega_{2\mathrm{pd}} = 0$ corresponds to the standard longitudinal readout with no squeezing.

With the output field $\hat{a}_{s,\mathrm{out}}(t) = \hat{a}_{s,\mathrm{in}}(t) + \sqrt{\kappa_s}\hat{a}_s(t)$ [S11], the output quadrature, carrying information about the qubit state and measured by a homodyne setup with a detection angle ϕ_h, is given by

$$\hat{\mathcal{Z}}_{\mathrm{out}}(t) = \hat{a}_{s,\mathrm{out}}(t)\, e^{-i\phi_h} + \hat{a}_{s,\mathrm{out}}^{\dagger}(t)\, e^{i\phi_h}. \tag{S46}$$

To evaluate the SNR, which is an essential parameter quantifying the homodyne detection, we define the following measurement operator,

$$\hat{M} = \sqrt{\kappa_s} \int_0^{\tau} dt\, \hat{\mathcal{Z}}_{\mathrm{out}}(t), \tag{S47}$$

where τ is the measurement time. Its average, $\langle \hat{M} \rangle$, is the qubit-state-dependent measurement signal, while the variance of the noise operator $\hat{M}_N = \hat{M} - \langle \hat{M} \rangle$ represents the measurement noise. Then, the SNR reads

$$\mathrm{SNR} = \frac{\left| \langle \hat{M} \rangle_{\uparrow} - \langle \hat{M} \rangle_{\downarrow} \right|}{\sqrt{\langle \hat{M}_N^2 \rangle_{\uparrow} + \langle \hat{M}_N^2 \rangle_{\downarrow}}}, \tag{S48}$$

where the arrows $\uparrow$ and $\downarrow$ refers to the excited and ground states of the qubit.

Note that the longitudinal coupling in fact offers a qubit-state-dependent resonant driving for the signal mode $\hat{a}_s$, and can act as an internal measurement tone. In this case, the input measurement tone is no longer needed, such that the average of the input operator $\hat{a}_{s,\mathrm{in}}(t)$ equals zero, i.e., $\langle \hat{a}_{s,\mathrm{in}}(t) \rangle = 0$, and then the correlations for $\hat{a}_{s,\mathrm{in}}(t)$ are given by

$$\langle \hat{a}_{s,\mathrm{in}}(t)\, \hat{a}_{s,\mathrm{in}}^{\dagger}(t') \rangle = \delta(t-t'), \tag{S49}$$

$$\langle \hat{a}_{s,\mathrm{in}}^{\dagger}(t)\, \hat{a}_{s,\mathrm{in}}(t') \rangle = \langle \hat{a}_{s,\mathrm{in}}(t)\, \hat{a}_{s,\mathrm{in}}(t') \rangle = 0. \tag{S50}$$

Under the initial condition $\langle \hat{a}_s(0)\rangle = 0$, we find

$$\langle \hat{M}\rangle_\uparrow - \langle \hat{M}\rangle_\downarrow = \frac{8\chi_z\kappa_s}{\left(\kappa_s^2 - 16\Omega_{2\mathrm{pd}}^2\right)^2}\Big\{ \left[\kappa_s^2(2-\kappa_s\tau) + 16(2+\kappa_s\tau)\Omega_{2\mathrm{pd}}^2\right]\sin(\phi_h-\phi_z) - 4\Omega_{2\mathrm{pd}}\left[\kappa_s(4-\kappa_s\tau) + 16\Omega_{2\mathrm{pd}}^2\tau\right]\cos(\phi_h+\phi_z-2\phi_{2\mathrm{pd}})\Big\} + \mathcal{F}_- e^{-\frac{1}{2}(\kappa_s-4\Omega_{2\mathrm{pd}})\tau} + \mathcal{F}_+ e^{-\frac{1}{2}(\kappa_s+4\Omega_{2\mathrm{pd}})\tau}, \tag{S51}$$

with

$$\mathcal{F}_\pm = \frac{8\chi_z\kappa_s}{(\kappa_s \pm 4\Omega_{2\mathrm{pd}})^2}\left[\cos(\phi_h+\phi_z-2\phi_{2\mathrm{pd}}) \pm \sin(\phi_h-\phi_z)\right]. \tag{S52}$$

Here, we have assumed $t_0 = 0$ for simplicity.

Furthermore, the quantum fluctuation of the output field $\hat{a}_{s,\mathrm{out}}(t)$, given by $\hat{f}_{\mathrm{out}}(t) = \hat{a}_{s,\mathrm{out}}(t) - \langle \hat{a}_{s,\mathrm{out}}(t)\rangle$, is found to be

$$\hat{f}_{\mathrm{out}}(t) = \hat{a}_{s,\mathrm{in}}(t) - \kappa_s\int_{-\infty}^{t} ds\cosh\left[2\Omega_{2\mathrm{pd}}(t-s)\right]e^{-\kappa_s(t-s)/2}\hat{a}_{s,\mathrm{in}}(s) + ie^{i2\phi_{2\mathrm{pd}}}\kappa_s\int_{-\infty}^{t} ds\sinh\left[2\Omega_{2\mathrm{pd}}(t-s)\right]e^{-\kappa_s(t-s)/2}\hat{a}_{s,\mathrm{in}}^\dagger(s). \tag{S53}$$

Here, we have assumed that before the measurement starts (i.e., the longitudinal qubit-field coupling starts), the system (i.e., the semiclassical DPA) is already in the steady state. Thus in Eq. (S53), the lower limit of integration has been extended to $-\infty$. The measurement noise, when expressed in terms of $\hat{f}_{\mathrm{out}}(t)$, is

$$\langle \hat{M}_N^2\rangle = \kappa_s\int_0^\tau\int_0^\tau dt_1dt_2\Big[\langle \hat{f}_{\mathrm{out}}^\dagger(t_1)\hat{f}_{\mathrm{out}}(t_2)\rangle + \langle \hat{f}_{\mathrm{out}}(t_1)\hat{f}_{\mathrm{out}}^\dagger(t_2)\rangle + \langle \hat{f}_{\mathrm{out}}(t_1)\hat{f}_{\mathrm{out}}(t_2)\rangle e^{-i2\phi_h} + \langle \hat{f}_{\mathrm{out}}^\dagger(t_1)\hat{f}_{\mathrm{out}}^\dagger(t_2)\rangle e^{i2\phi_h}\Big], \tag{S54}$$

and after a straightforward but tedious calculation is found as follows:

$$\langle \hat{M}_N^2\rangle = \kappa_s\tau + \frac{16\kappa_s^2\Omega_{2\mathrm{pd}}}{\left(\kappa_s^2 - 16\Omega_{2\mathrm{pd}}^2\right)^3}\Big\{\left[\kappa_s^3(2-\kappa_s\tau) + 32\left(3\kappa_s + 8\Omega_{2\mathrm{pd}}^2\tau\right)\Omega_{2\mathrm{pd}}^2\right]\sin\left[2(\phi_h-\phi_{2\mathrm{pd}})\right] - 8\kappa_s^2(3-\kappa_s\tau)\Omega_{2\mathrm{pd}} - 128(1+\kappa_s\tau)\Omega_{2\mathrm{pd}}^3\Big\} + \mathcal{Z}_- e^{-\frac{1}{2}(\kappa_s-4\Omega_{2\mathrm{pd}})\tau} - \mathcal{Z}_+ e^{-\frac{1}{2}(\kappa_s+4\Omega_{2\mathrm{pd}})\tau}, \tag{S55}$$

where

$$\mathcal{Z}_\pm = \frac{16\kappa_s^2\Omega_{2\mathrm{pd}}}{(\kappa_s \pm 4\Omega_{2\mathrm{pd}})^3}\left\{1 \pm \sin\left[2(\phi_h-\phi_{2\mathrm{pd}})\right]\right\}. \tag{S56}$$

From Eq. (S55) the noise is minimized by choosing $\phi_h - \phi_{2\mathrm{pd}} = \pi/4$, corresponding to the homodyne detection along the direction of squeezing. Then according to Eq. (S51), the signal separation $\left|\langle \hat{M}\rangle_\uparrow - \langle \hat{M}\rangle_\downarrow\right|$ is maximized for $\phi_h - \phi_z = \pi/2$.

For these optimal phases, below we discuss the SNR. Let us first consider a special case of $\Omega_{2\mathrm{pd}} = 0$, corresponding to the standard longitudinal readout with no squeezing. In such a case, the SNR is given by [S12]

$$\mathrm{SNR}_z^{\mathrm{std}} = \frac{6}{\kappa_s\tau}\mathrm{SNR}_x^{\mathrm{std}} = \chi_z\tau\sqrt{2\kappa_s\tau}, \tag{S57}$$

for a short-time measurement (i.e., $\kappa_s\tau \ll 1$). Here, $\mathrm{SNR}_x^{\mathrm{std}} = \varepsilon(\kappa_s\tau)^{5/2}/(3\sqrt{2}\kappa_s)$ refers to the short-time SNR of the standard dispersive readout with a measurement tone of amplitude ε [S13]. For comparison, we have assumed

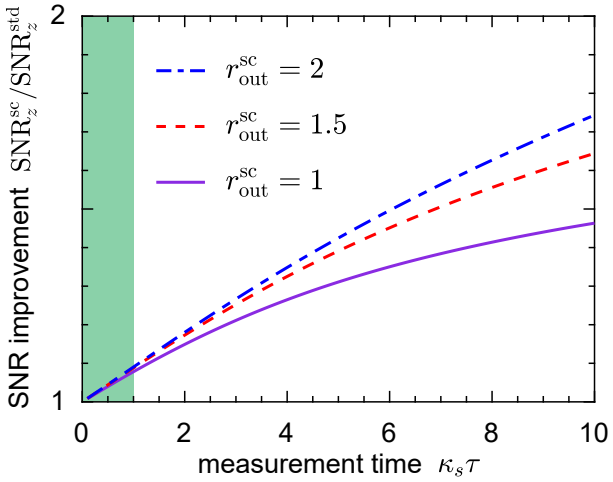

FIG. S4. SNR improvement, i.e., $\mathrm{SNR}_z^{\mathrm{sc}}/\mathrm{SNR}_z^{\mathrm{std}}$, of longitudinal qubit readout using intracavity squeezing of the semiclassical degenerate parametric amplifier for $r_{\mathrm{out}}^{\mathrm{sc}} = 1$, 1.5, and 2. The SNR is calculated using Eqs. (S51) and (S55) for $\phi_h = \phi_{2\mathrm{pd}} + \pi/4 = \phi_z + \pi/2$. The green shaded area refers to the regime of most interest in experiments.

the amplitude ε to be equal to the longitudinal coupling strength χ_z. Clearly, the longitudinal readout requires much shorter measurement times, compared to the dispersive readout.

We now consider the SNR for any $\Omega_{2\mathrm{pd}}$ that can keep the system stable, i.e., $\Omega_{2\mathrm{pd}} < \kappa_s/2$. For the short-time measurement, i.e., $\kappa_s\tau \ll 1$ or $(\kappa_s \pm 4\Omega_{2\mathrm{pd}}) \ll 1$, the signal separation is found to be

$$\left|\langle\hat{M}\rangle_{\uparrow} - \langle\hat{M}\rangle_{\downarrow}\right| \simeq 2\chi_z\kappa_s\tau^2, \tag{S58}$$

up to second order, and likewise, the measurement noise is reduced to

$$\langle\hat{M}_N^2\rangle \simeq \kappa_s\tau - \frac{4\Omega_{2\mathrm{pd}}}{\kappa_s + 4\Omega_{2\mathrm{pd}}}(\kappa_s\tau)^2 \simeq \kappa_s\tau. \tag{S59}$$

We find that both the short-time signal and noise are almost unaffected by the two-photon driving $\Omega_{2\mathrm{pd}}$ or equivalently by intracavity squeezing. In turn, the optimal SNR is found to be

$$\mathrm{SNR}_z^{\mathrm{sc}} \simeq \mathrm{SNR}_z^{\mathrm{std}}. \tag{S60}$$

This implies that the semiclassical-DPA intracavity squeezing does not improve the SNR for the short-time measurement. In Fig. S4, we plot the SNR improvement, i.e., the ratio $\mathrm{SNR}_z^{\mathrm{sc}}/\mathrm{SNR}_z^{\mathrm{std}}$, as a function of the measurement time $\kappa_s\tau$. In this figure, we define the parameter

$$r_{\mathrm{out}}^{\mathrm{sc}} = \ln\left(\frac{\kappa_s + 4\Omega_{2\mathrm{pd}}}{\kappa_s - 4\Omega_{2\mathrm{pd}}}\right), \tag{S61}$$

which characterizes the degree of squeezing of the output field of the semiclassical DPA in the absence of the qubit. It can be seen that the SNR is almost unaffected in the regime $\tau \leq 1/\kappa_s$, which is of most interest in experiments.

Moreover, for the long-time measurement, i.e., $\kappa_s\tau \gg 1$ or $(\kappa_s \pm 4\Omega_{2\mathrm{pd}}) \gg 1$, an exponential improvement in the SNR can be obtained as

$$\mathrm{SNR}_z^{\mathrm{sc}} \simeq \frac{\kappa_s}{\kappa_s + 4\Omega_{2\mathrm{pd}}} \exp\left(r_{\mathrm{out}}^{\mathrm{sc}}\right) \mathrm{SNR}_z^{\mathrm{std}}. \tag{S62}$$

For example, choosing $r_{\mathrm{out}}^{\mathrm{sc}} = 2$ ($\simeq 17$ dB) can give a more than four-fold improvement in the long-time limit. However, as shown in Fig. S4, even with a long measurement time of up to $\tau = 10/\kappa_s$, the output-field squeezing of $r_{\mathrm{out}}^{\mathrm{sc}} = 2$ can only lead to a modest improvement of the SNR by a factor of $\simeq 1.7$. This means that in order to obtain the exponential improvement given in Eq. (S62), the measurement time needs to be extremely long, which is infeasible in experiments. Hence, the semiclassical-DPA intracavity squeezing *cannot* significantly improve the SNR during a practically feasible measurement time, even with a strong output-field squeezing.

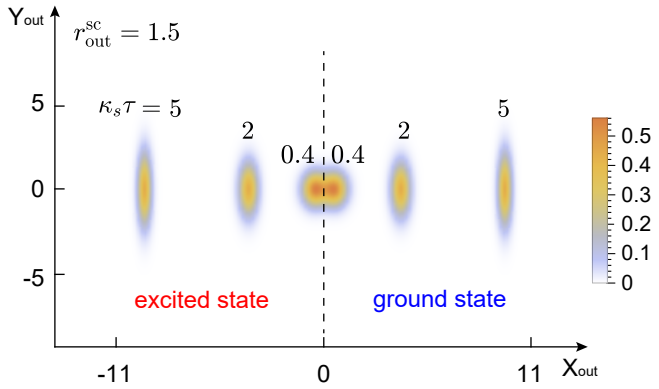

FIG. S5. Phase-space representation of longitudinal qubit readout using intracavity squeezing of the semiclassical degenerate parametric amplifier. We chose, for $r_{\rm out}^{\rm sc} = 1.5$ ($\simeq 13$ dB), three different measurement times: $\kappa_s\tau = 0.4$, 2, and 5. The resulting Wigner functions on the left and right of the vertical dashed line correspond to the excited and ground states of the qubit, respectively. The degree of squeezing of the measurement noise strongly depends on the measurement time.

To understand this result of no significant improvement of practical interest in experiments, we now turn to phase space. In order to describe the Wigner function of the output field, we define the temporal mode [S14, S15]

$$\hat{A} = \frac{1}{\sqrt{\tau}} \int_0^\tau dt\, \hat{a}_{s,\rm out}\,(t)\,. \tag{S63}$$

The resulting bosonic commutation relation $\left[\hat{A}, \hat{A}^\dagger\right] = 1$ allows us to introduce two conjugate quadratures,

$$\hat{X}_{\rm out} = \frac{1}{2}\left(\hat{A} + \hat{A}^\dagger\right), \quad \text{and} \quad \hat{Y}_{\rm out} = \frac{1}{2i}\left(\hat{A} - \hat{A}^\dagger\right), \tag{S64}$$

which satisfy $\left[\hat{X}_{\rm out}, \hat{Y}_{\rm out}\right] = i$. With these quadratures, the Wigner function of the output field can be calculated as

$$W\left(X_{\rm out}, Y_{\rm out}\right) = \frac{1}{2\pi\sqrt{\rm Det\,(\mathbf{D})}} \exp\left(-\frac{1}{2}\mathbf{G}^{\rm T}\mathbf{D}^{-1}\mathbf{G}\right), \tag{S65}$$

where

$$\mathbf{G} = \left(X_{\rm out} - \langle\hat{X}_{\rm out}\rangle, Y_{\rm out} - \langle\hat{Y}_{\rm out}\rangle\right)^{\rm T}, \tag{S66}$$

$$\mathbf{D} = \begin{pmatrix} \langle\hat{X}_{\rm out}^2\rangle - \langle\hat{X}_{\rm out}\rangle^2 & \langle\hat{X}_{\rm out}\hat{Y}_{\rm out} + \hat{Y}_{\rm out}\hat{X}_{\rm out}\rangle/2 - \langle\hat{X}_{\rm out}\rangle\langle\hat{Y}_{\rm out}\rangle \\ \langle\hat{X}_{\rm out}\hat{Y}_{\rm out} + \hat{Y}_{\rm out}\hat{X}_{\rm out}\rangle/2 - \langle\hat{X}_{\rm out}\rangle\langle\hat{Y}_{\rm out}\rangle & \langle\hat{Y}_{\rm out}^2\rangle - \langle\hat{Y}_{\rm out}\rangle^2 \end{pmatrix}. \tag{S67}$$

We show in Fig. S5 the Wigner functions in phase space for different measurement times and for the ground and excited states of the qubit. The degree of squeezing of the measurement noise increases from the initial value zero as the measurement time increases, and then tends asymptotically towards the limit value $r_{\rm out}^{\rm sc}$. The practically unsqueezed measurement noise in the regime $\kappa_s\tau \leq 1$ is the physical reason for almost no improvement in the SNR for the short-time measurement.

S7. Improved longitudinal qubit readout using our fully-quantum-DPA intracavity squeezing

Following the same method as in Sec. S6, we here derive and analyze the measurement signal, measurement noise, and SNR for the longitudinal readout of a qubit embedded in the fully quantum DPA. In our approach, the qubit is coupled to the pump mode, rather than to the signal mode as described in Sec. S6. We demonstrate that, compared to the case of using the semiclassical-DPA intracavity squeezing, *our fully-quantum-DPA intracavity squeezing enables an exponential improvement in the SNR for any measurement time, thus yielding a faster and higher-SNR (i.e., higher-fidelity) qubit readout.*

With the Hamiltonian $\hat{H}_z^{\rm fq}$ in Eq. (14) in the main article, the quantum Langevin equations of motion for the modes $\hat{a}_p$ and $\hat{\beta}_s$ are

$$\dot{\hat{a}}_p = -i\sigma\chi_z e^{i\phi_z} - i\left(G_-\hat{\beta}_s + G_+\hat{\beta}_s^\dagger\right) - \frac{\kappa_p}{2}\hat{a}_p - \sqrt{\kappa_p}\hat{a}_{p,\rm in}(t), \tag{S68}$$

$$\dot{\hat{\beta}}_s = -i\left(G_-\hat{a}_p + G_+\hat{a}_p^\dagger\right) - \frac{\kappa_s}{2}\hat{\beta}_s - \sqrt{\kappa_s}\hat{\beta}_{s,\rm in}. \tag{S69}$$

As was assumed for the generation of the strong steady-state intracavity squeezing, the photon loss rate κ_s of the mode $\hat{\beta}_s$ is sufficiently large, such that we can set $\dot{\hat{\beta}}_s = 0$ to adiabatically eliminate the mode $\hat{\beta}_s$. This leads to the following adiabatic equation of motion for the mode $\hat{a}_p$,

$$\dot{\hat{a}}_p = -i\sigma\chi_z e^{i\phi_z} - \frac{\kappa}{2}\hat{a}_p - \sqrt{\kappa}\hat{\mathcal{A}}_{\rm in}(t). \tag{S70}$$

Here, the noise operator $\hat{\mathcal{A}}_{\rm in}(t) = \frac{1}{\sqrt{\kappa}}\left[\sqrt{\kappa_p^{\rm ad}}\hat{a}_{p,\rm in}^{\rm ad}(t) + \sqrt{\kappa_p}\hat{a}_{p,\rm in}(t)\right]$ describes the overall input noise. The pump mode $\hat{a}_p$ is then found, after formally integrating, to be

$$\begin{aligned}\hat{a}_p(t) = {} & e^{-\kappa(t-t_0)/2}\hat{a}_p(t_0) \\ & - i\frac{2}{\kappa}\sigma\chi_z e^{i\phi_z}\left[1 - e^{-\kappa(t-t_0)/2}\right] - \sqrt{\kappa}\int_{t_0}^{t} e^{-\kappa(t-s)/2}\hat{\mathcal{A}}_{\rm in}(s)\,ds.\end{aligned} \tag{S71}$$

As mentioned in Sec. S6, the longitudinal coupling can be thought of as an internal measurement tone, and there is no input or external measurement tone. In this case, $\langle\hat{\beta}_{s,\rm in}(t)\rangle = \langle\hat{\mathcal{A}}_{\rm in}(t)\rangle = 0$. Moreover, the correlations for $\hat{\beta}_{s,\rm in}(t)$, which approximately describe the vacuum noise of the mode $\hat{\beta}_s$, are

$$\langle\hat{\beta}_{s,\rm in}(t)\,\hat{\beta}_{s,\rm in}^\dagger(t')\rangle = \delta(t-t'), \tag{S72}$$

$$\langle\hat{\beta}_{s,\rm in}^\dagger(t)\,\hat{\beta}_{s,\rm in}(t')\rangle = \langle\hat{\beta}_{s,\rm in}(t)\,\hat{\beta}_{s,\rm in}(t')\rangle = 0, \tag{S73}$$

and, as a consequence, the correlations for $\hat{\mathcal{A}}_{\rm in}(t)$ are

$$\langle\hat{\mathcal{A}}_{\rm in}(t)\,\hat{\mathcal{A}}_{\rm in}^\dagger(t')\rangle = \left[\frac{1}{4\mathcal{C}+1} + \frac{4\mathcal{C}}{4\mathcal{C}+1}\cosh^2(r_p)\right]\delta(t-t'), \tag{S74}$$

$$\langle\hat{\mathcal{A}}_{\rm in}^\dagger(t)\,\hat{\mathcal{A}}_{\rm in}(t')\rangle = \frac{4\mathcal{C}}{4\mathcal{C}+1}\sinh^2(r_p)\,\delta(t-t'), \tag{S75}$$

$$\langle\hat{\mathcal{A}}_{\rm in}(t)\,\hat{\mathcal{A}}_{\rm in}(t')\rangle = -\frac{2\mathcal{C}}{4\mathcal{C}+1}\sinh(2r_p)\,\delta(t-t'). \tag{S76}$$

Here, $\mathcal{C} = \mathcal{G}^2/(\kappa_s\kappa_p)$ is the cooperativity of the DPA. It is seen that the correlation in Eq. (S74) includes two contributions, one from the natural photon loss of the pump mode $\hat{a}_p$ and the other from the adiabatic effect of the signal Bogoliubov mode $\hat{\beta}_s$.

It follows, according to the input-output relation $\hat{\mathcal{A}}_{\rm out}(t) = \hat{\mathcal{A}}_{\rm in}(t) + \sqrt{\kappa}\hat{a}_p(t)$, that the signal separation is found to be

$$\left|\langle\hat{M}\rangle_\uparrow - \langle\hat{M}\rangle_\downarrow\right| = 8\chi_z\tau\left|\sin(\phi_h - \phi_z)\right|\left\{1 - \frac{2}{\kappa\tau}\left[1 - \exp(-\kappa\tau/2)\right]\right\}. \tag{S77}$$

Here, we have assumed $t_0 = 0$ as usual. This signal separation is the same as obtained in the standard longitudinal readout with no squeezing [S12, S16]. Moreover, the quantum fluctuation noise of the output field now is $\hat{f}_{\rm out}(t) = \hat{\mathcal{A}}_{\rm out}(t) - \langle\hat{\mathcal{A}}_{\rm out}(t)\rangle$, and evolves as

$$\hat{f}_{\rm out}(t) = \hat{\mathcal{A}}_{\rm in}(t) - \kappa\int_{-\infty}^{t}\exp\left[-\kappa(t-s)/2\right]\hat{\mathcal{A}}_{\rm in}(s)\,ds. \tag{S78}$$

Here, the lower limit of integration has been extended to $-\infty$ for the same reason as mentioned in Sec. S6. The expression of the measurement noise is the same as in Eq. (S54) but now replacing $\kappa_s \mapsto \kappa$, and, then, a straightforward calculation leads to

$$\langle\hat{M}_N^2\rangle = \kappa\tau\left\{\frac{1}{4\mathcal{C}+1} + \frac{4\mathcal{C}}{4\mathcal{C}+1}\left[\cosh(2r_p) - \cos(2\phi_h)\sinh(2r_p)\right]\right\}. \tag{S79}$$

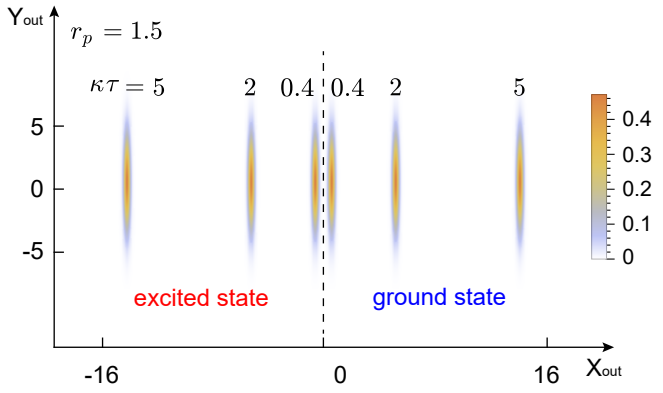

FIG. S6. Phase-space representation of longitudinal qubit readout using intracavity squeezing of the fully quantum degenerate parametric amplifier. We chose, for $r_{\rm out} = 1.5$ ($\simeq 13$ dB), three different measurement times: $\kappa\tau = 0.4$, 2, and 5. The resulting Wigner functions on the left and right of the vertical dashed line correspond to the excited and ground states of the qubit, respectively. The strong squeezing of the measurement noise is independent of the measurement time.

As long as $\mathcal{C} \gg e^{2r_p}/4$, then $\langle \hat{M}_N^2 \rangle$ is reduced to the measurement noise of the longitudinal readout with injecting a squeezed reservoir in the ideal case of no transmission and injection losses [S12], i.e.,

$$\langle \hat{M}_N^2 \rangle_{\rm ideal} = \kappa\tau \left[\cosh\left(2r_p\right) - \cos\left(2\phi_h\right)\sinh\left(2r_p\right)\right]. \tag{S80}$$

By choosing $\phi_z = \pi/2$ and $\phi_h = 0$, the optimal SNR of the longitudinal readout using the fully-quantum-DPA intracavity squeezing is given by

$$\mathrm{SNR}_z^{\rm fq} = \sqrt{\frac{4\mathcal{C}+1}{4\mathcal{C}\exp\left(-2r_p\right)+1}}\,\mathrm{SNR}_z^{\rm std}, \tag{S81}$$

which shows a significant improvement in the SNR. In particular, an exponential improvement,

$$\mathrm{SNR}_z^{\rm fq} \simeq \exp\left(r_p\right)\mathrm{SNR}_z^{\rm std}, \tag{S82}$$

can be achieved for $\mathcal{C} \gg e^{2r_p}/4$. We note that Eqs. (S81) and (S82) hold for *any* measurement time. This is because the degree of squeezing of the measurement noise, i.e., $\langle \hat{M}_N^2 \rangle/\kappa\tau$, is independent of the measurement time τ [see Eq. (S79)], and particularly is equal to the degree of intracavity squeezing for $\phi_h = 0$, i.e., $\langle \hat{M}_N^2 \rangle/\kappa\tau = \left(\xi_p^2\right)_{\rm ss} = \left[1 + 4\mathcal{C}\exp\left(-2r_p\right)\right]/\left(1+4\mathcal{C}\right)$. This becomes more apparent in phase space shown in Fig. S6. We find that a short measurement time of $\tau = 0.4/\kappa$ can well resolve the measurement signals associated with the ground and excited states of the qubit. This is in stark contrast to what we have already shown in Fig. S5, where the same measurement time (i.e., $\tau = 0.4/\kappa_s$) leads to a high degree of overlap of the measurement signals, such that they cannot be resolved. In order to compare, we here have assumed κ_s in Fig. S5 and κ in Fig. S6 to be equal. Thus, our approach can enable a faster and higher-SNR qubit readout.

S8. Possible implementations of our approach for improving longitudinal qubit readout

The longitudinal qubit-field coupling can be directly realized via circuit design in circuit quantum electrodynamics [S17–S23]. Alternatively, some synthetic approaches, e.g., strongly driving the qubit-field dispersive coupling, have also been proposed and even demonstrated in experiments [S16, S24–S28]. In this section, as an example, we discuss in detail a possible implementation of the Hamiltonian $\hat{H}_z^{\rm fq}$ in Eq. (14) in a synthetic manner. In particular, we refer to the experimental implementation reported in Ref. [S27], where the longitudinal coupling is synthesized with driving the qubit at the cavity frequency.

Let us now assume that the qubit is driven with phase ϕ_z, amplitude $\mathcal{E}_q^{\rm d}$, and frequency $\omega_q^{\rm d}$. The total Hamiltonian accordingly is given, in the frame rotating at ω_d, by

$$\begin{aligned}\hat{H}_T = \hat{H} &+ \frac{1}{2}\Delta_q\hat{\sigma}_z + g_q\left(\hat{\sigma}_-\hat{a}_p^\dagger + \mathrm{H.c.}\right)\\ &+ \mathcal{E}_q^{\rm d}\left[e^{i\phi_z}\hat{\sigma}_- e^{-i\left(\omega_d-\omega_q^{\rm d}\right)t} + \mathrm{H.c.}\right],\end{aligned} \tag{S83}$$

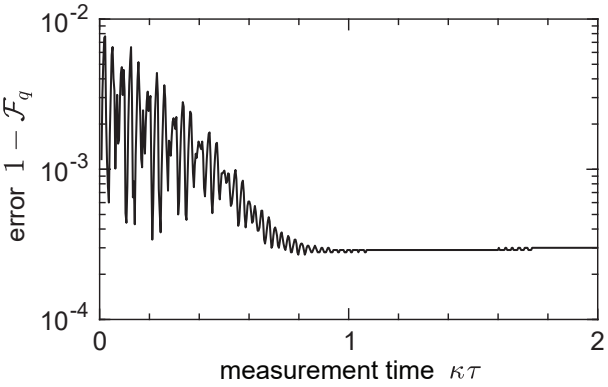

FIG. S7. State error, $1-\mathcal{F}_q$, as a function of the measurement time $\kappa\tau$. We assumed that $g_q = g$, $\mathcal{E}_q^{\rm d} = 10g_q$, $\phi_z = \pi/2$, $\Delta_q^{\rm d} = 200g_q$, $\Delta_q = \Delta_q^{\rm d} + \Delta_p$, $G_+ = 0.7G_-$, and other parameters associated with $\hat{H}_{\rm eff}$ are the same as those in Fig. 1(b). We assumed that the qubit is initially in the state $(|g\rangle + |e\rangle)/\sqrt{2}$, while the signal and pump modes are in the steady state given by $\hat{H}_{\rm eff}$.

where $\hat{H}$ has been given in the main article, $\hat{\sigma}_\pm$ are the raising/lowering operators of the qubit, g_q is the strength of the coupling of the qubit to the pump mode, and $\Delta_q = \omega_q - \omega_d$ is the detuning of the qubit from the driving of the pump mode. We follow the same procedure listed in Sec. S3 to find that the dynamics of the total system can be described by the following Hamiltonian

$$\begin{aligned}\hat{H}_T' = \hat{H}_{\rm eff} &+ g_q\left(\hat{\sigma}_-\hat{a}_p^\dagger e^{-i\Delta_q^{\rm d}t} + {\rm H.c.}\right)\\ &+ \mathcal{E}_q^{\rm d}\left(\hat{\sigma}_- e^{i\phi_z}e^{-i\Delta_q^{\rm d}t} + {\rm H.c.}\right)\\ &+ g_q\alpha_p^{\rm d}\left(\hat{\sigma}_- e^{-i\Delta_q t} + {\rm H.c.}\right).\end{aligned} \tag{S84}$$

Here, we have assumed that $\omega_q - \omega_p = \omega_q - \omega_q^{\rm d} = \Delta_q^{\rm d}$. Note that the detuned driving of the qubit, which is associated with the field amplitudes α_p induced by the $\omega_\pm^{\rm d}$ drivings of the signal mode, have been neglected since $\alpha_p \ll \alpha_p^{\rm d}$.

We further assume $\Delta_q^{\rm d} \gg \{g_q, \mathcal{E}_q^{\rm d}\}$ and $\Delta_q \gg g_q\alpha_p^{\rm d}$, justifying for a perturbative treatment of the second, third and fourth terms of $\hat{H}_T'$ using the formalism of Ref. [S2]. We then find that

$$\hat{H}_T' \approx \hat{H}_{\rm eff} + \chi_z\hat{\sigma}_z\left(\hat{a}_p e^{-i\phi_z} + \hat{a}_p^\dagger e^{i\phi_z}\right) + \chi_x\hat{a}_p^\dagger\hat{a}_p\hat{\sigma}_z, \tag{S85}$$

where

$$\chi_z = \mathcal{E}_q^{\rm d}g_q/\Delta_q^{\rm d}, \quad \text{and} \quad \chi_x = g_q^2/\Delta_q^{\rm d} \tag{S86}$$

are the strengths of the longitudinal and dispersive couplings between the qubit and the pump mode, respectively. In Eq. (S85), we have subtracted the term describing the resonance shift of the qubit, i.e., $\frac{1}{2}\delta_z\hat{\sigma}_z$, where

$$\delta_z = \left[g_q^2 + 2\left(\mathcal{E}_q^{\rm d}\right)^2\right]/\Delta_q^{\rm d} + 2\left(g_q\alpha_p^{\rm d}\right)^2/\Delta_q. \tag{S87}$$

This is because this term can be completely eliminated in a proper frame. Under the assumption of $\mathcal{E}_p^{\rm d} \gg g_q$, the longitudinal coupling χ_z is much stronger than the dispersive coupling χ_x, so that the latter can be neglected, yielding

$$\hat{H}_T' \simeq \hat{H}_{\rm eff} + \chi_z\hat{\sigma}_z\left(\hat{a}_p e^{-i\phi_z} + \hat{a}_p^\dagger e^{i\phi_z}\right). \tag{S88}$$

This is the Hamiltonian $\hat{H}_z^{\rm fq}$ in Eq. (14) in the main article.

To confirm the validity of Eq. (S88), we perform numerical simulations, as shown in Fig. S7. Specifically, we calculate the fidelity, $\mathcal{F}_q$, of two qubit states that are given by the evolution under the two Hamiltonians in Eqs. (S84) and (S88), respectively, from the same initial state. In Fig. S7, we assume that the initial state of the qubit is $(|g\rangle + |e\rangle)/\sqrt{2}$. At the same time, the initial state of the signal and pump modes is assumed to be the steady state given by $\hat{H}_{\rm eff}$, indicating that when the measurement starts, a steady-state squeezing has already been generated. It can be seen in Fig. S7 that during a long measurement time, the state error, $1-\mathcal{F}_q$, can be kept well below 10^{-2} for some modest parameters.

[S1] S. Chaturvedi, K. Dechoum, and P. D. Drummond, "Limits to squeezing in the degenerate optical parametric oscillator," Phys. Rev. A **65**, 033805 (2002).

[S2] O. Gamel and D. F. V. James, "Time-averaged quantum dynamics and the validity of the effective Hamiltonian model," Phys. Rev. A **82**, 052106 (2010).

[S3] Z. Leghtas *et al.*, "Confining the state of light to a quantum manifold by engineered two-photon loss," Science **347**, 853 (2015).

[S4] S. Touzard *et al.*, "Coherent Oscillations inside a Quantum Manifold Stabilized by Dissipation," Phys. Rev. X **8**, 021005 (2018).

[S5] R. Lescanne, M. Villiers, T. Peronnin, A. Sarlette, M. Delbecq, B. Huard, T. Kontos, M. Mirrahimi, and Z. Leghtas, "Exponential suppression of bit-flips in a qubit encoded in an oscillator," Nat. Phys. **16**, 509 (2020).

[S6] C. W. S. Chang, C. Sabín, P. Forn-Díaz, F. Quijandría, A. M. Vadiraj, I. Nsanzineza, G. Johansson, and C. M. Wilson, "Observation of three-photon spontaneous parametric down-conversion in a superconducting parametric cavity," Phys. Rev. X **10**, 011011 (2020).

[S7] A. Vrajitoarea, Z. Huang, P. Groszkowski, J. Koch, and A. A Houck, "Quantum control of an oscillator using a stimulated Josephson nonlinearity," Nat. Phys. **16**, 211 (2020).

[S8] X. Guo, C.-L. Zou, and H. X. Tang, "Second-harmonic generation in aluminum nitride microrings with 2500%/W conversion efficiency," Optica **3**, 1126–1131 (2016).

[S9] A. W. Bruch, X. Liu, J. B. Surya, C.-L. Zou, and H. X. Tang, "On-chip $\chi^{(2)}$ microring optical parametric oscillator," Optica **6**, 1361–1366 (2019).

[S10] J.-Q. Wang, Y.-H. Yang, M. Li, X.-X. Hu, J. B. Surya, X.-B. Xu, C.-H. Dong, G.-C. Guo, H. X. Tang, and C.-L. Zou, "Efficient Frequency Conversion in a Degenerate $\chi^{(2)}$ Microresonator," Phys. Rev. Lett. **126**, 133601 (2021).

[S11] C. W. Gardiner and M. J. Collett, "Input and output in damped quantum systems: Quantum stochastic differential equations and the master equation," Phys. Rev. A **31**, 3761–3774 (1985).

[S12] N. Didier, J. Bourassa, and A. Blais, "Fast Quantum Nondemolition Readout by Parametric Modulation of Longitudinal Qubit-Oscillator Interaction," Phys. Rev. Lett. **115**, 203601 (2015).

[S13] X. Wang, A. Miranowicz, and F. Nori, "Ideal Quantum Nondemolition Readout of a Flux Qubit without Purcell Limitations," Phys. Rev. Applied **12**, 064037 (2019).

[S14] I. Strandberg, G. Johansson, and F. Quijandría, "Wigner negativity in the steady-state output of a Kerr parametric oscillator," Phys. Rev. Research **3**, 023041 (2021).

[S15] Y. Lu, I. Strandberg, F. Quijandría, G. Johansson, S. Gasparinetti, and P. Delsing, "Propagating Wigner-Negative States Generated from the Steady-State Emission of a Superconducting Qubit," Phys. Rev. Lett. **126**, 253602 (2021).

[S16] S. Touzard, A. Kou, N. E. Frattini, V. V. Sivak, S. Puri, A. Grimm, L. Frunzio, S. Shankar, and M. H. Devoret, "Gated Conditional Displacement Readout of Superconducting Qubits," Phys. Rev. Lett. **122**, 080502 (2019).

[S17] Y.-x. Liu *et al.*, "Controllable Coupling between Flux Qubits," Phys. Rev. Lett. **96**, 067003 (2006).

[S18] A. J. Kerman, "Quantum information processing using quasiclassical electromagnetic interactions between qubits and electrical resonators," New J. Phys. **15**, 123011 (2013).

[S19] P.-M. Billangeon, J. S. Tsai, and Y. Nakamura, "Circuit-QED-based scalable architectures for quantum information processing with superconducting qubits," Phys. Rev. B **91**, 094517 (2015).

[S20] P.-M. Billangeon, J. S. Tsai, and Y. Nakamura, "Scalable architecture for quantum information processing with superconducting flux qubits based on purely longitudinal interactions," Phys. Rev. B **92**, 020509(R) (2015).

[S21] S. Richer and D. DiVincenzo, "Circuit design implementing longitudinal coupling: A scalable scheme for superconducting qubits," Phys. Rev. B **93**, 134501 (2016).

[S22] S. Richer, N. Maleeva, S. T. Skacel, I. M. Pop, and D. DiVincenzo, "Inductively shunted transmon qubit with tunable transverse and longitudinal coupling," Phys. Rev. B **96**, 174520 (2017).

[S23] R. Stassi and F. Nori, "Long-lasting quantum memories: Extending the coherence time of superconducting artificial atoms in the ultrastrong-coupling regime," Phys. Rev. A **97**, 033823 (2018).

[S24] J. Q. You and F. Nori, "Quantum information processing with superconducting qubits in a microwave field," Phys. Rev. B **68**, 064509 (2003).

[S25] A. Blais, J. Gambetta, A. Wallraff, D. I. Schuster, S. M. Girvin, M. H. Devoret, and R. J. Schoelkopf, "Quantum-information processing with circuit quantum electrodynamics," Phys. Rev. A **75**, 032329 (2007).

[S26] A. Eddins, S. Schreppler, D. M. Toyli, L. S. Martin, S. Hacohen-Gourgy, L. C. G. Govia, H. Ribeiro, A. A. Clerk, and I. Siddiqi, "Stroboscopic Qubit Measurement with Squeezed Illumination," Phys. Rev. Lett. **120**, 040505 (2018).

[S27] J. Ikonen, J. Goetz, J. Ilves, A. Keränen, A. M. Gunyho, M. Partanen, K. Y. Tan, D. Hazra, L. Grönberg, V. Vesterinen, S. Simbierowicz, J. Hassel, and M. Möttönen, "Qubit Measurement by Multichannel Driving," Phys. Rev. Lett. **122**, 080503 (2019).

[S28] R. Dassonneville *et al.*, "Fast High-Fidelity Quantum Nondemolition Qubit Readout via a Nonperturbative Cross-Kerr Coupling," Phys. Rev. X **10**, 011045 (2020).